Zhao *et al. Chem. Synth.* **2025**, *5*, 32
DOI: 10.20517/cs.2024.14

Chemical Synthesis

Review

Open Access

Recent advances in conjugated ladder-type porous polymer networks for rechargeable batteries

Cunhang Zhao[1,2,#], Jie Yan[2,#], Zijiu Ma[2], Yalin Zhang[2], Tu Hu[1,*], Haitao Zhang[2,*]

[1]Faculty of Metallurgical and Energy Engineering, Kunming University of Science and Technology, Kunming 650093, Yunnan, China.
[2]Beijing Key Laboratory of Ionic Liquids Clean Process, Institute of Process Engineering, Chinese Academy of Sciences, Beijing 100190, China.
[#]Authors contributed equally.

[*]**Correspondence to:** Prof. Haitao Zhang, Beijing Key Laboratory of Ionic Liquids Clean Process, Institute of Process Engineering, Chinese Academy of Sciences, 1 North 2nd Street, Zhongguancun, Beijing 100190, China. E-mail: htzhang@ipe.ac.cn; Prof. Tu Hu, Faculty of Metallurgical and Energy Engineering, Kunming University of Science and Technology, No. 253, Xuefu Road, Wuhua District, Kunming 650093, Yunnan, China. E-mail: hutu1219@126.com

How to cite this article: Zhao, C.; Yan, J.; Ma, Z.; Zhang, Y.; Hu, T.; Zhang, H. Recent advances in conjugated ladder-type porous polymer networks for rechargeable batteries. *Chem. Synth.* **2025**, *5*, 32. https://dx.doi.org/10.20517/cs.2024.14

Received: 31 Jan 2024 **First Decision:** 19 Jul 2024 **Revised:** 1 Aug 2024 **Accepted:** 12 Aug 2024 **Published:** 10 Mar 2025

Academic Editor: Xiang-Dong Yao **Copy Editor:** Pei-Yun Wang **Production Editor:** Pei-Yun Wang

Abstract

Owing to the abundant resources, environmental benignity, structural designability, and reasonable theoretical capacity, organic electrode compounds are considered to be an excellent substitute for traditional inorganic electrode materials, which can be applied in green and sustainable recharge batteries. Consequently, organic electrode materials have received considerable attention over the past decade, and numerous organic and polymeric materials have been prepared as high-efficiency electrode materials for batteries. Among them, conjugated ladder-type porous polymer networks (PPNs) with intralayer π-conjugation, interlayer π-π stacking interactions, and rigid backbones have emerged as attractive platforms for rechargeable batteries. This review summarizes the linkage chemistry, synthesis methods, and typical structure of ladder PPNs, the redox activity of the linkage, and their applications in secondary batteries. Further, approaches to enhance the performance and efficiency of these electrode materials are presented. The potential battery applications of the ladder PPNs structure are also discussed.

Keywords: Conjugated ladder polymer networks, synthetic method, rechargeable batteries

INTRODUCTION

The increasing global efforts to reduce our carbon footprint have raised the demand for green and

sustainable electrochemical energy storage technologies[1]. The active materials of electrodes in conventional metal-ion batteries are mainly inorganic transition metal oxides and graphite, which are derived from scarce and nonrenewable resources. By contrast, organic electrode materials consist of light elements (e.g., C, H, O, N, and S) and can be derived from biomass. Furthermore, these materials have the advantages of abundant resources, environmental compatibility, structural designability, and reasonable theoretical capacity, making them a powerful alternative to traditional inorganic electrode compounds and promising candidates for green and sustainable recharge batteries[2-9]. With good structural flexibility, some organic electrode materials can accommodate large counter-cations without space constraints. Consequently, these materials have drawn great attention in the area of rechargeable batteries. Various types of organic electrode materials, including small redox molecules (e.g., organic radical compounds[10], organodisulfides[11], carbonyl compounds[12], azo compounds[13], imine compounds[14], and carboxylate compounds[15]), linear polymers[16,17] (e.g., conductive polymers and conjugated polymers), and polymeric networks [e.g., covalent organic frameworks (COFs)[18,19] and porous organic polymers (POPs)[20,21]], have been extensively investigated in electrochemical energy storage.

Conjugated ladder polymers (cLPs) are a class of multiple-stranded polymers in which periodic linkages connect the strands resembling the rungs of a ladder, creating a series of contiguous rings that share at least two atoms, and the fused rings in the backbones are fully conjugated[22,23]. Due to their fused-ring backbone, cLPs exhibit admirable thermal and chemical stability. Further, their conjugated coplanar structure facilitates extended π-conjugation, rapid intra-chain charge transport, and strong π-π stacking interactions. The rigid ladder polymers are mainly linear polymers with poor solubility owing to their backbone rigidity and coplanarity. With the rapid progress of reticular chemistry, porous polymer networks (PPNs), such as COFs[24-28] and POPs[29-34], have drawn tremendous attention owing to their permanent porosity and outstanding structural, chemical, and functional diversity. POPs were a broad concept and could be categorized as crystalline and amorphous analogs according to the crystallinity degree. The crystalline analogs primarily belong to COFs. In contrast, the amorphous analogs can be divided into porous aromatic frameworks (PAFs), conjugated microporous polymers (CMPs), PPNs, porous graphitic frameworks (PGFs), *etc.* based on their structural features or synthetic methods. The repeat units of these polymer networks are typically connected through a single bond. With the advent of new ring annulation reactions, rigid polymer networks, which integrate the structural features of cLPs with those of COFs and POPs, have made significant progress in the last decade. Given the wide variety of categories in PPNs, we quote the reported concept of porous ladder polymer networks (ladder PPNs)[35] in this review to represent all the PPNs with ladder-type linkage and fully conjugated backbone to avoid confusion. The ladder PPNs materials [Figure 1] with intralayer π-conjugation, interlayer π-π stacking interactions, and rigid backbone exhibit remarkable properties, such as intrinsic conductivity, porosity, and thermal and chemical stability. What is more, most linkage of these networks was formed from heteroatom (O. N) engaged reaction, importing redox-active sites in the backbone. Extra redox-active sites could also be introduced to ladder PPNs by polymeric reaction of monomers based on redox-active moieties to form multi-redox active networks. With built-in redox-active moieties, a series of ladder PPNs have been synthesized and employed as electrode materials in organic batteries. The intrinsic conductivity ensures efficient charge transfer, improving the overall performance of the battery. The well-defined pore structure facilitates diffusion kineties, enabling efficient ion transport. In addition, the layered structure allows the intercalation of ions between the layers, enabling high-capacity energy storage. The energy storage performance of ladder PPNs electrode materials is summarized in Table 1.

For better electrochemical performance, the organic electrode materials must contain redox-active groups, such as C=O, C=N, C≡N, and N=N, which can combine with counter-cations to ensure a high

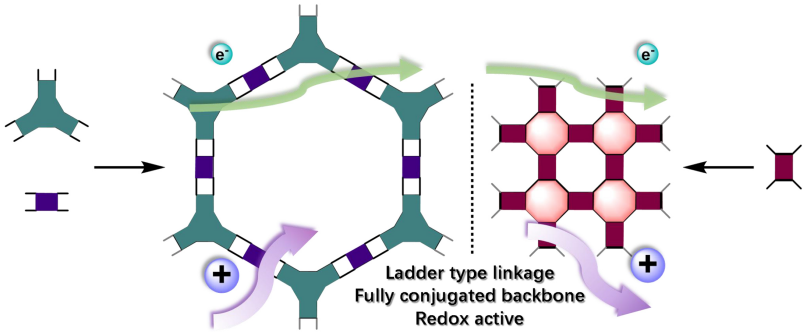

Figure 1. Graphical illustration of synthesis, structural feature and redox activity of Ladder PPNs. PPNs: Porous polymer networks.

capacity[9,36-39]. Ladder PPNs can be prepared by polycondensation of various well-designed organic monomers containing redox-active groups. In this review, we describe the recent advances in ladder PPNs, including the linkage chemistry, synthesis methods, typical structure, redox activity of the linkage, and their applications in secondary batteries. Further, strategies to prepare ladder PPNs-based high-efficiency electrode materials are presented, and their potential applications in rechargeable batteries are also discussed.

SYNTHESIS OF REDOX-ACTIVE LADDER PPNS AND THEIR APPLICATION IN RECHARGEABLE BATTERIES

As a specific subtype of ladder polymers, ladder PPNs are commonly prepared by two methods: single-step ladderization and two-step approach of polymerization followed by ladderization[22,35]. The single-step ladderization strategy is simpler and more accessible to low-cost materials. Consequently, we primarily focus on the single-step ladderization strategy for the synthesis of redox-active ladder PPNs, including the formation reaction of the fused linkage, redox activity, and the application of ladder PPNs in rechargeable batteries. The redox-active ladder PPNs are classified according to the fused linkage.

Hexaazatriphenylene networks

The compound 1,4,5,8,9,12-hexaazatriphenylene (HAT) is composed of three fused pyrazine rings, making it an electron-deficient, rigid, planar, and aromatic system. A less common HAT derivative is hexaazatrinaphthylene (HATN), which contains three fused quinoxalines. HAT and derivatives contain six imine functional groups as redox-active sites and are widely employed as active materials in secondary batteries. In 2017, Peng *et al.* revealed the charge transfer mechanism of HATN in lithium-ion batteries (LIBs) based on a two-step three-electron transfer process [Figure 2A and B][14]. Firstly, HATN was reduced to radical anions and chelated with lithium ions to form HATN-3Li intermediate in which the adjacent nitrogen atoms located in different pyrazine rings co-coordinated with one Li^+. Then, the intermediate HATN-3Li was reduced gradually to anions and each pair of adjacent nitrogen atoms chelated with another Li^+ ion to form HATN-6Li. A similar charge storage mechanism of HATN was also proposed for sodium-ion batteries (SIBs)[40].

HAT and derivatives have been well studied as electrode materials in rechargeable batteries, and the structures and applications of HAT-based organic electrode materials in different secondary batteries have been reviewed in a recent report[41]. The ladder PPNs with periodic HAT-based skeletons [Figure 2C] are considered to be an excellent platform for rechargeable batteries. The built-in HAT moieties serving as redox-active sites provide high capacity, while the highly π-conjugated skeleton combined with the permanent nano/micropores facilitate charge carrier dynamics.

Table 1. The summary of ladder PPNs electrode materials in the review

Ladder PPNs		Capacity (mAh·g^{-1}) @ current density (A·g^{-1})	Capacity retention [cycle number, current density (A·g^{-1})]	CE	Battery type	Ref.
HAT-B	NG-HCP	935@0.1; 665@0.5; 480@1; 341@1.7; 295@2; 257@2.3; 237@2.5	~100% (600, 1.2)	100%	LIB	[43]
	PGF-1	842@0.1; 480@0.5; 189@5	78.3% (400, 5)	99.95%	LIB	[44]
	Aza-COF	523@0.06; 374@0.6; 32@3; 161@6	87% (500, 3)	100%	SIB	[45]
HAT-BQ	BQ-COF	502.4@0.03; 198.4@1.54; 170.7@7.73	81% (1,000, 1.54)	100%	LIB	[46]
	TQBQ-COF	327.2@0.1; 278.6@0.3; 234@1; 180.6@5; 134.3@10	89% (500, 0.1) 91.3% (1,000, 0.5) 96.4% (1,000, 1)	~100%	SIB	[47]
		423@0.03; 363@0.15; 329@0.3; 185@3	90.9% (600, 0.9) 58% (2,000, 0.9)	99.5%	PIB	[48]
	TB-COF	253@1; 224@2; 207@3; 188@5; 164@10; 140@20; 124@30; 113@40; 108@50; 105@60; 104@70	69.9% (3,000, 5)	~100%	CIB	[49]
HAT-P	HAT-P/pRGO	285@0.1; 319@0.2; 285@0.3; 250@0.4; 211@0.5; 165@1; 119@2; 88@4	~100% (1,600, 0.5)	/	LIB	[50]
	PA-COF	265@0.05; 234@0.1; 202@0.2; 176@0.5; 153@1; 125@2; 93@5; 68@10	62% (10,000, 1)	99.62%	ZIS	[51]
C2N	C_2N-450	/	~100% (500, 0.372)	~99.5%	LIB	[54]
	PCN-350	351@0.03; 296@0.15; 241@1.6; 151@3; 95@6	88.5% (6,500, 0.6)	99.5%	SIB	[55]
	HAT-CQP-800	/	82.3% (510, 0.8)	/	LIB	[56]
HAT-TP	HAT-TP/NGA-CMP400	874.3@0.1; 406.1@2.5	~100% (500, 1)	99%	LIB	[53]
F-CQN-1-600		186@0.1; 167@0.2; 152@0.5; 142@1; 129@2; 105@5	95.8% (2,000, 2)	99.95%	LIB	[58]
QPP-FAC-Pc-COF		424@0.05; 368@0.1; 279@0.3; 241@0.5; 205@1; 173@2	~100% (10,000, 0.2)	100%	PIB	[60]
BB-FAC-Pc-COF		333@0.05; 270@0.1; 178@0.3; 150@0.5; 119@1; 92@2	~100% (6,000, 0.2)	/	PIB	
2DBBL-TP		71@10; 69@20; 65@40; 60@100; 51@200	~100% (10,000, 100)	100%	ZIB	[71]
BQ*b*TPL		152.9@0.1; 125.6@0.2; 109.3@0.5; 97.3@1	94.8% (1,500, 1)	/	LIB	[75]

PPNs: Porous polymer networks; CE: coulombic efficiency; HAT: hexaazatriphenylene-hexacarbonitrile; NG-HCP: nitrogen-rich graphene-like holey conjugated polymers; LIB: lithium-ion battery; PGF: porous graphitic framework; COF: covalent organic framework; SIB: sodium-ion battery; BQ: benzoquinone; PIB: potassium-ion battery; CIB: calcium-ion battery; pRGO: partially reduced graphene oxide; PA: phenanthrolin; ZIS: zinc-ion storage; PCN: polymeric carbon nitride; CQP: covalent quinazoline polymer; TP: triphenylene; NGA: novel 2D graphene analogue; F-CQN: fluorinated covalent quinazoline network; QPP: quinoxalino[2′,3′:9,10]phenanthro[4,5-abc]phenazine; FAC: fully aromatic conjugated.

HAT and derivatives can be obtained by condensation reaction between hexaketocyclohexane (HKH) and (Z)-ethene-1,2-diamine or ortho-phenylenediamine derivative [Figure 2D], which is commonly employed as the linkage reaction to form HAT-based ladder PPNs. The nitrogen-rich two-dimensional (2D) graphene-like networks can be prepared from HKH and bi- or tri-functional ortho-phenylenediamine molecules. A less common method to prepare HAT-based ladder PPNs is an ortho-dinitrile triple condensation of a pre-aligned HAT precursor via direct carbonization procedure [Figure 2D][42]. Until now, only one HAT network C-HAT-CN with an empirical formula of C_2N has been prepared via ortho-dinitrile triple condensation of hexaazatriphenylene-hexacarbonitrile (HAT-CN). The HATN-CN molecule was

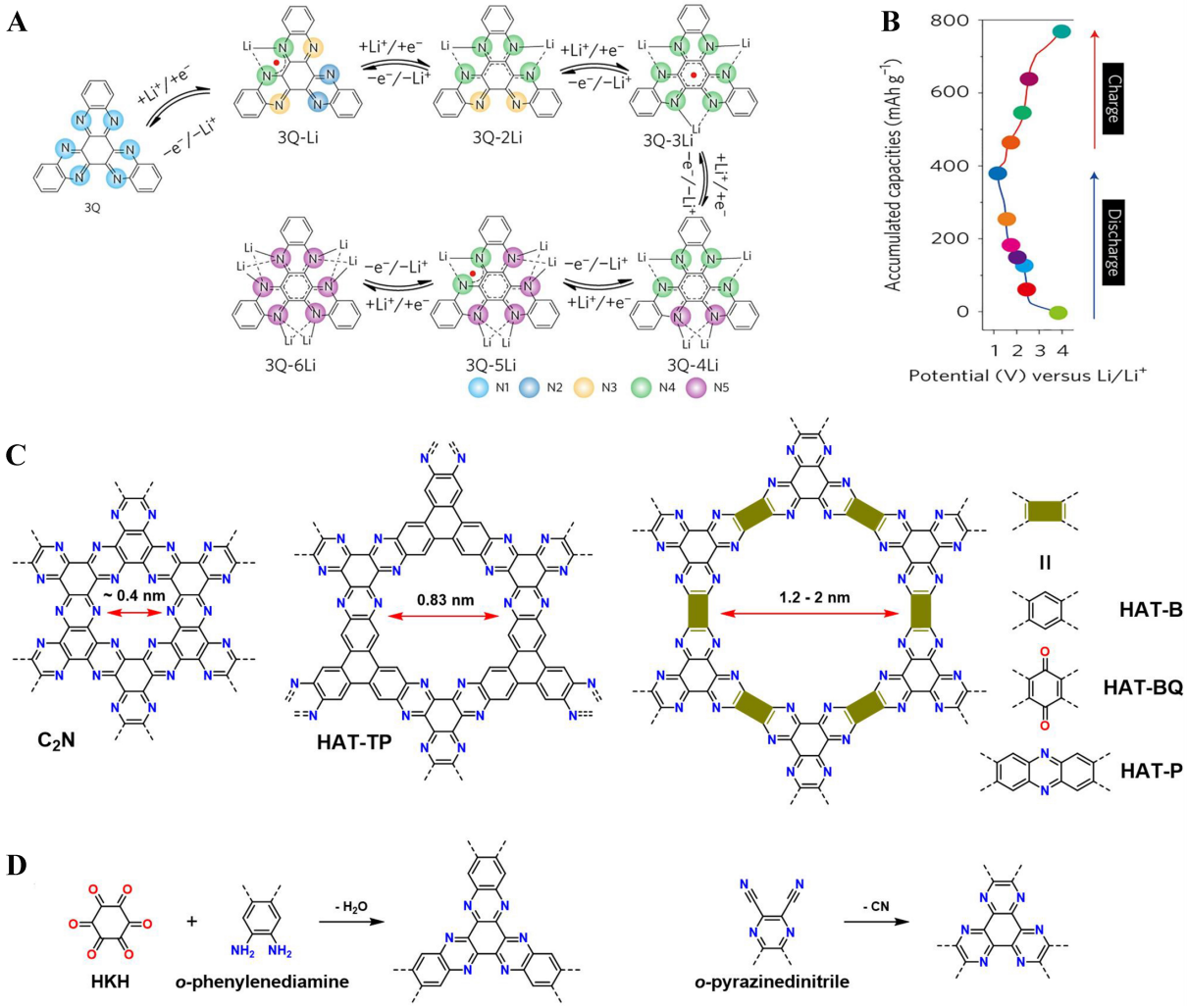

Figure 2. (A) Predicted structural evolution of HAT (3Q)-nLi$^+$ in the discharge process[14]; (B) The galvanostatic charge and discharge curve of HATN at 20 mA g^{-1}[14]; (C) Structures of representative HAT networks with redox activity; (D) Formation reaction of HAT linkage. Reproduced from: (A and B) Peng *et al.*(2017), Nature Publishing Group[14].HAT: Hexaazatriphenylene; HATN: hexaazatrinaphthylene.

directly heated to a temperature of 550, 700, 850, and 1,000 °C without any pretreatment. The specific surface area of these materials could reach 1,000 m^2·g^{-1}. It is noteworthy that with the elevated synthesis temperature from 550 to 850 °C, the nitrogen content of the C-HAT-CN materials dramatically decreased to 4.9%, while the specific surface area increased slightly. The formation of HAT linkage and the representative HAT-based ladder PPNs, which can be used as electrodes for rechargeable batteries [Figure 2C and D].

In 2017, Lin *et al.* synthesized an amorphous HAT network: a free-standing single-layer nanosheet of a nitrogen-rich graphene-like holey conjugated polymer (NG-HCP, empirical formula: C_5HN_2), by a solution-processed condensation reaction of HKH and 1,2,4,5-Tetraaminobenzene (TAB) with sulfuric acid catalysis[43]. The electrical conductivity of NG-HCP in the pellet reached 3.55 × 10^{-2} S·cm^{-1}. The single-layer NG-HCP nanosheets were obtained via a methanesulfonic acid (MSA)-based solution assembly process. The NG-HCP nanosheets as the active anode material for LIBs offered a reversible capacity of 1,015 mAh·g^{-1} at 0.1 A·g^{-1} (0-3.0 V *vs.* Li$^+$/Li), while the pristine NG-HCP for anodes displayed a reversible capacity of less

than 300 mAh·g^{-1}. Nano-engineering has been established as a feasible strategy for performance improvement of electrode materials for rechargeable batteries. The nanostructured NG-HCP confirmed the good exposure of active sites in the nanosheets and ensured better combination with the conductive additive carbon nanotube (CNT), which are conducive to effective lithium storage and improved electrical conductivity. In 2020, by replacing the acidic conditions with basic hydrothermal conditions, the crystalline HAT network PGF-1 (HAT-B) was obtained from HKH and TAB, which was then used as the LIB cathode[44]. The crystalline 2D network with a pore diameter of 1.2-1.3 nm was arranged in eclipsed (AA) staking pattern to form a well-defined channel. The PGF-1 cathode delivered capacities of 842 mAh·g^{-1} at 100 mA·g^{-1} (1-3.6 V *vs.* Li$^+$/Li) and 189 mAh·g^{-1} at 5,000 mA·g^{-1}, respectively [Figure 3A-C][44]. The contrast amorphous counterpart displayed much lower capacities of 263 and 128 mAh·g^{-1} at 100 and 5,000 mA·g^{-1}. Furthermore, PGF-1 cathodes exhibited better cycling stability with 78.3% capacity retention over 1,400 cycles at 500 mA·g^{-1}, while the amorphous counterpart [amorphous polymers (AP-1)] cathode with lower capacity decayed sharply from 236 to 176 mAh·g^{-1} over 400 cycles [Figure 3A-C][44]. During the lithiation process, lithium ions bounded with pyrazine nitrogen atoms and intercalated in the layered structure with the carbon species. The electrochemical lithium storage was strengthened by the improved crystallinity with improved structural regularity, which facilitated more exposed active sites for lithium storage and continuous channels for ion transport in the network. Shehab *et al.* synthesized the crystalline HAT network Aza-COF (same structure as PGF-1) under acidic conditions, which was demonstrated to be an excellent anode material for SIBs[45]. The Aza-COF-based SIB delivered a high average specific capacity and reasonable cycling stability, indicating its immense application potential in rechargeable batteries.

Introducing multi-active sites while reducing the electrochemically inactive parts is an effective approach to design organic electrode materials with excellent theoretical capacity. Wu *et al.* and Shi *et al.* immobilized benzoquinones into the HAT network to form a ladder PPN with multi-redox active sites of C=N and C=O[46,47]. The HAT network HAT-benzoquinone (BQ) containing crystalline benzoquinone (empirical formula: C_5ON_2) was synthesized from HKH and tetraminobenzoquinone (TABQ) under acidic conditions. With all C=N and C=O groups serving as redox-active sites, the HAT-BQ network offered an outstanding theoretical capacity of 773 mAh·g^{-1}. The calculated pore size of the 2D porous structure was 1.39 nm. However, this network tended to stack in slipped-parallel patterns with shaded pores. The electric conductivity of this fully conjugated HAT-BQ network was 10^{-9}-10^{-8} S·cm^{-1}. The conductive network has been employed as a cathode material in LIBs and SIBs, and as an anode material in potassium-ion batteries (PIBs), which delivered specific capacities of 502.4 mAh·g^{-1} (at 39 mA·g^{-1}, 1.2-3.5 V *vs.* Li$^+$/Li), 452.0 mAh·g^{-1} (at 20 mA·g^{-1}, 1-3.6 V *vs.* Na$^+$/Na), and 423.0 mAh·g^{-1} (at 30 mA·g^{-1}, 0-3 V *vs.* K$^+$/K), respectively [Figure 4A-C][46-48]. Even at large current densities of 7.7 A·g^{-1} (for LIBs), 10.0 A·g^{-1} (for SIBs), and 3.0 A·g^{-1} (for PIBs), the HAT-BQ network still offered high specific capacities of 170.7, 134.3, and 185 mAh·g^{-1}, respectively, showing great rate capability [Figure 4D-F][46-48]. Furthermore, the stable network showed impressive long-term cycling stability with capacity retentions of 81% and 96.4% after 1,000 cycles in LIBs (at 1.54 A·g^{-1}) and SIBs (at 1 A·g^{-1}) and 58% after 2,000 cycles in PIBs (at 0.9 A·g^{-1}) [Figure 4G-I][46-48]. The graphene-like HAT-BQ network was also used as a host material for NH_4^+ ions in an aqueous battery and exhibited a high specific NH_4^+ capacity of 220.4 mAh·g^{-1} at 0.5 A·g^{-1}. The quinone carbonyl oxygen and pyrazine nitrogen offer H-bond reaction to NH_4^+ ions, resulting in suitable NH_4^+ ion host behavior. Recently, the HAT-BQ network (TB-COF) was also applied in calcium-ion batteries (CIBs) for cation storage which delivered a high reversible capacity of 253 mAh·g^{-1} at 1.0 A·g^{-1} (-1.0-0.6 V *vs.* Ag/AgCl) and cycling stability showing a 0.01% capacity decay per cycle at 5 A·g^{-1} during 3,000 cycles[49]. Calcium ions with large ionic radius prefer to load at interlamination sites of HAT-BQ network, and the redox-active C=O, C=N and infrequent C=C groups were involved in the intercalation process.

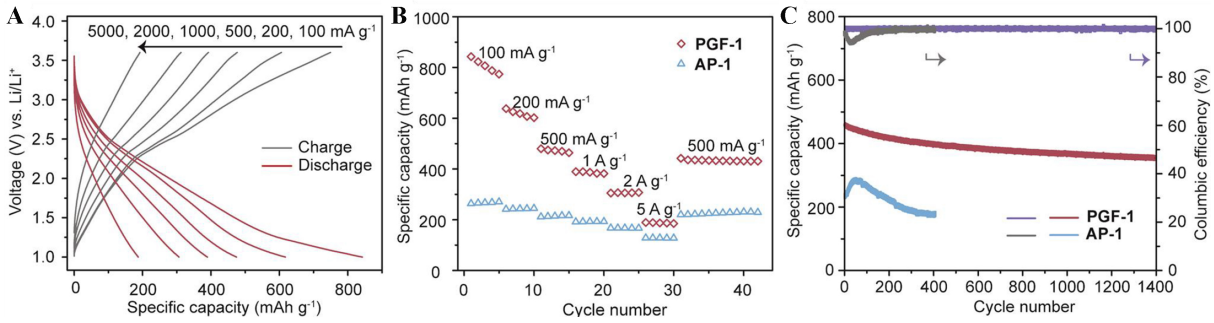

Figure 3. Electrochemical performance comparison of crystalline PGF-1 and amorphous AP-1 as cathode materials for LIBs. (A) Charge and discharge curves of PGF-1 at various current densities; (B) Rate capabilities of PGF-1 and AP-1 with various current densities; (C) Cycling stability of PGF-1 and AP-1[44]. Reproduced from: Li *et al.* (2020), Cell Publishing Group[44]. PGF: Porous graphitic framework; AP-1: amorphous polymers; LIBs: lithium-ion batteries.

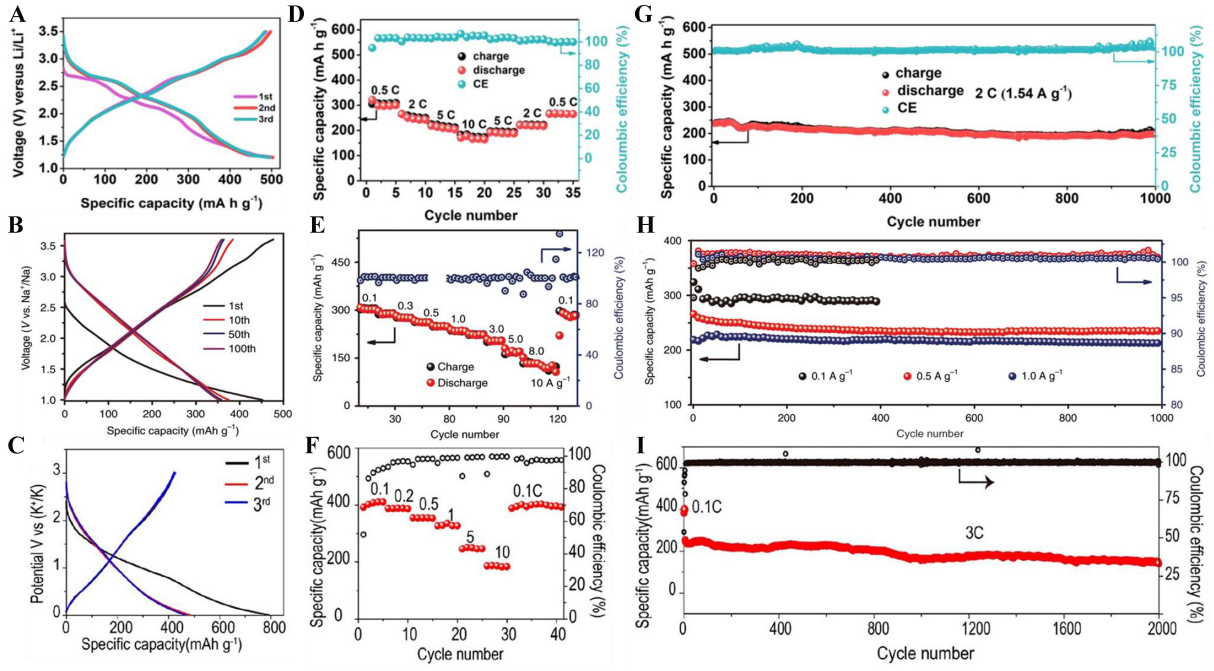

Figure 4. The capacity-voltage profile of HAT-BQ for LIB with (A) different current densities (39 mA·g^{-1}), (B) SIB (20 mA·g^{-1}) and (C) PIB (at a current density of 30 mA·g^{-1}); Rate capabilities of HAT-BQ with various current rates for (D) LIB, (E) SIB and (F) PIB; Cycling stability of HAT-BQ in (G) LIB (at 1.54 A·g^{-1}), (H) SIB (at 1 A·g^{-1}) and (I) PIB (at 0.9 A·g^{-1})[46-48]. Reproduced from: (A, D, G) Wu *et al.* (2020), ScienceDirect[46]; (B, E, H) Shi *et al.* (2020), Nature Publishing Group[47]; (C, F, I) Chen *et al.* (2023), American Chemical Society[48]. HAT: Hexaazatriphenylene; BQ: benzoquinone; LIB: lithium-ion battery; SIB: sodium-ion battery; PIB: potassium-ion battery.

The HAT-based ladder PPNs with expanded hexagonal 2D lattices were obtained from a larger bifunctional ortho-phenylenediamine monomer. By replacing the 1,2,4,5-benzenetetraamine (BTA) with 2,3,6,7-tetraaminophenazine (TAP), a HAT network (HAT-P) containing phenazine with a simulated pore size of 2 nm was prepared via polycondensation between HKH and TAP[50,51]. The amorphous HAT-P (empirical formula: $C_8H_2N_3$) network was synthesized through homogeneous reaction with a sulfuric acid catalyst in 1-methyl-2-pyrrolidinone (NMP) solution, which served as a cathode material in LIBs[50]. The maximum capacity of HAT-P cathodes reached 630 mAh·g^{-1} at 0.05 A·g^{-1} (1.2-4 V *vs.* Li$^+$/Li) after 70 charge/recharge cycles, while the first-cycle capacity was 406 mAh·g^{-1}[50]. The significant improvement of Li$^+$ capacity was mainly attributed to the redispersion of aggregated HATN-P particles to small particles, resulting in a

homogeneous distribution of active materials on the surface of a conductive additive [partially reduced graphene oxide (pRGO)], which eventually facilitated electron and ion transfer. The crystalline HAT-P COF was synthesized under solvothermal conditions with ethylene glycol/pyridine/mesitylene solution and showed a medium pore size of 2-5 nm. With the large pore structure facilitating reversible mobile ion intercalation, HAT-P COF was employed as a cathode in an aqueous zinc-ion storage (ZIS) device and provided a capacity of 247 $mAh \cdot g^{-1}$ at 0.1 $A \cdot g^{-1}$ (0.2-1.6 V *vs.* Zn^{2+}/Zn) and cycling stability with 0.38% capacity decay per cycle over 10,000 cycles at 1 $A \cdot g^{-1}$ [Figure 5][51].

Tri-functional ortho-phenylenediamine monomers, hexaaminobenzene (HAB), and 2,3,6,7,10,11-triphenylenehexaamine (HATP) have also been employed to prepare HAT network[52,53]. An HAT network C_2N (named according to the empirical formula) with a simulated pore size of ~0.4 nm was synthesized from HAB and HKH via wet-chemical reaction [Figure 6A], and the C_2N material was further annealed at 450 °C to get C_2N-450, which was applied as an anode material in LIBs[54]. Due to the improvement in the conductivity and crystallinity by the annealing procedure, C_2N-450 offered a superior reversible capacity of 395.1 $mAh \cdot g^{-1}$ at 372 $mA \cdot g^{-1}$ (0.02-3 V *vs.* Li^+/Li) [Figure 6B], but its cycling stability and rate capability were unsatisfactory. Recently, Yan *et al.* examined the influence of annealing temperature on the performance of C_2N as a high-efficiency electrode material for SIBs[55]. A reliable moderate pyrolysis strategy has been proven to be effective in preparing a high-performance HAT polymer anode for SIBs. The C_2N-350 (polymeric carbon nitride, PCN-350) obtained by the pyrolysis of C_2N at 350 °C delivered a high Na^+ storage capacity of 351 $mAh \cdot g^{-1}$ at 30 $mA \cdot g^{-1}$ (0-3 V *vs.* Na^+/Na), superior rate capability of 95 $mAh \cdot g^{-1}$ at 6 $A \cdot g^{-1}$, and ultra-stable cyclability with capability retention of 88.5% over 6,500 cycles at 600 $mA \cdot g^{-1}$ [Figure 6C and D]. Such moderate pyrolysis reduced the optical bandgap (from 1.33 to 1.15 eV) and ensured high nitrogen content residue, improving the electronic conductivity (10^{-5} $S \cdot cm^{-1}$) and ensuring abundant redox-active sites in the C_2N material. The C_2N material (named HAT-CQP) synthesized via ortho-dinitrile triple condensation of HAT-CN [Figure 6E] with excellent porosity provided excellent Li storage performance[56], which was superior to that of the C_2N analog prepared via a wet-chemistry process. The use of HAT-CQP as an anode material in LIBs offered a high capacity of 581 $mAh \cdot g^{-1}$ at 800 $mA \cdot g^{-1}$ (0.01-3 V *vs.* Li^+/Li), which was still maintained at 478 $mAh \cdot g^{-1}$ after 500 cycles (82.3% capacity retention) [Figure 6F]. The polycondensation reaction between HATP and HKH produced a HAT network HAT-triphenylene (TP) (empirical formula: C_4HN) with a simulated pore size of 0.8 nm[53]. The heat-treated HAT-TP exhibited a high surface area (521.3 $m^2 \cdot g^{-1}$, 17.6 times that of the pristine network) and served as an anode material, delivering a high reversible capacity of 701 $mAh \cdot g^{-1}$ at 1 $A \cdot g^{-1}$ (0-3 V *vs.* Li^+/Li) and retaining 406.1 $mAh \cdot g^{-1}$ at 2.5 $A \cdot g^{-1}$.

The HAT-linked ladder PPNs have been well researched in the field of secondary batteries, and numerous HAT networks with modified pore size and multi-redox active sites have been synthesized. The enhancement in the electrochemical performance of HAT-based ladder PPNs electrode materials has been explored from the perspective of nano-engineering and moderate pyrolysis strategy. A high surface area, suitable pore size, abundant redox-active sites, and high electrical conductivity are crucial to achieving good electrochemical performance of ladder PPNs for rechargeable batteries.

Tricycloquinazoline networks

Tricycloquinazoline (TQ) is a large, electron-deficient, nitrogen-rich aromatic molecule. Buyukcakir *et al.* first employed the trimerization of aromatic ortho-aminonitriles to produce a series of TQ networks, called covalent quinazoline networks (CQNs), under ionothermal conditions of $ZnCl_2$ [Figure 7][57]. CQNs showed layered structure, microporous features, and excellent thermal stability up to 500 °C. The surface area and pore size distribution of the CQNs could be controlled by the synthesis temperature and the amount of the catalyst. An excessive concentration of $ZnCl_2$ (10 equivalents versus monomer) and a high temperature

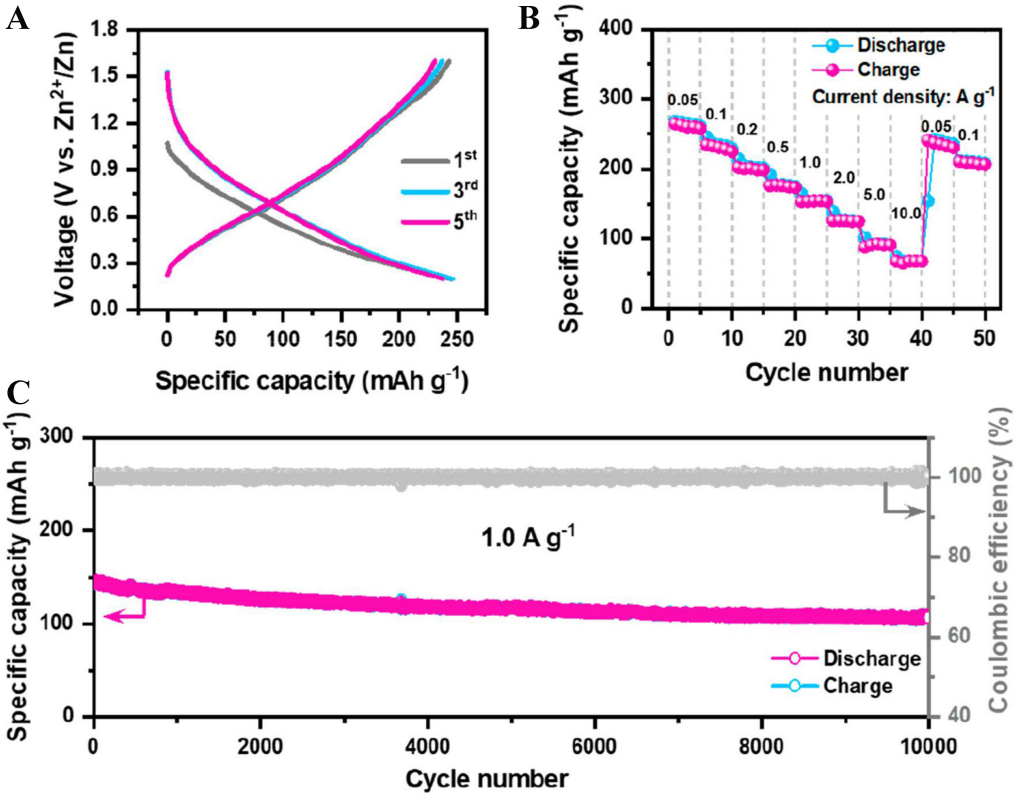

Figure 5. (A) Charge and discharge curve, (B) rate capability and (C) cycling stability of HAT-P COF as a cathode in ZIS[51]. Reproduced from: Wang *et al.* (2020), American Chemical Society[51]. HAT: Hexaazatriphenylene; COF: covalent organic framework; ZIS: zinc-ion storage.

reaching 400 °C resulted in the highest Brunauer-Emmett-Teller (BET) surface area of 1,870 $m^2 \cdot g^{-1}$. The nitrogen-rich backbone, layered structure, porosity, and stability make CQNs a potential candidate for electrode materials of batteries.

In 2021, Yang *et al.* prepared various nanoporous fluorinated CQNs (F-CQNs) as cathode materials using fluorinated aromatic aminonitrile precursors for LIBs via an ionothermal approach [Figure 7][58]. The introduction of fluorine species led to a much easier synthetic procedure of monomer compared with its non-fluorinated counterpart. The extended π-conjugated backbone, high content of nitrogen, and high surface area of F-CQNs synergistically improved the energy storage capacity. The surface area and total pore volume of F-CQNs rose with temperature. Further, the nitrogen content slightly dropped with the increase in reaction temperature from 400 to 600 °C but sharply decreased when the temperature reached 700 °C. The F-CQNs-600 synthesized under 600 °C showed high surface areas (1.581 $m^2 \cdot g^{-1}$) and high content of nitrogen (23.49 wt.%), resulting a good cathode performance for LIBs with a high capacity of 250 $mAh \cdot g^{-1}$ at 0.1 $A \cdot g^{-1}$, high-rate capability of 105 $mAh \cdot g^{-1}$ at 5.0 $A \cdot g^{-1}$ [Figure 8A][58], and good cycling stability with 95.8% capacity retention over 2,000 cycles at 2.0 $A \cdot g^{-1}$ [Figure 8B][58]. The ladder PPNs materials containing TQ moieties can effectively improve the storage capacity of lithium, providing ideas for the development of organic electrode materials with reliable and excellent performance for electrochemical energy storage.

In 2021, Yan *et al.* studied the storage mechanism of lithium in TQ[59]. Nine-electron-related redox activity with Li^+ was identified via experimental characterization and theoretical calculations. Three Li^+ ions were bound with the three pyrimidine N atoms and three Li^+ ions located around the central N atom and C=C

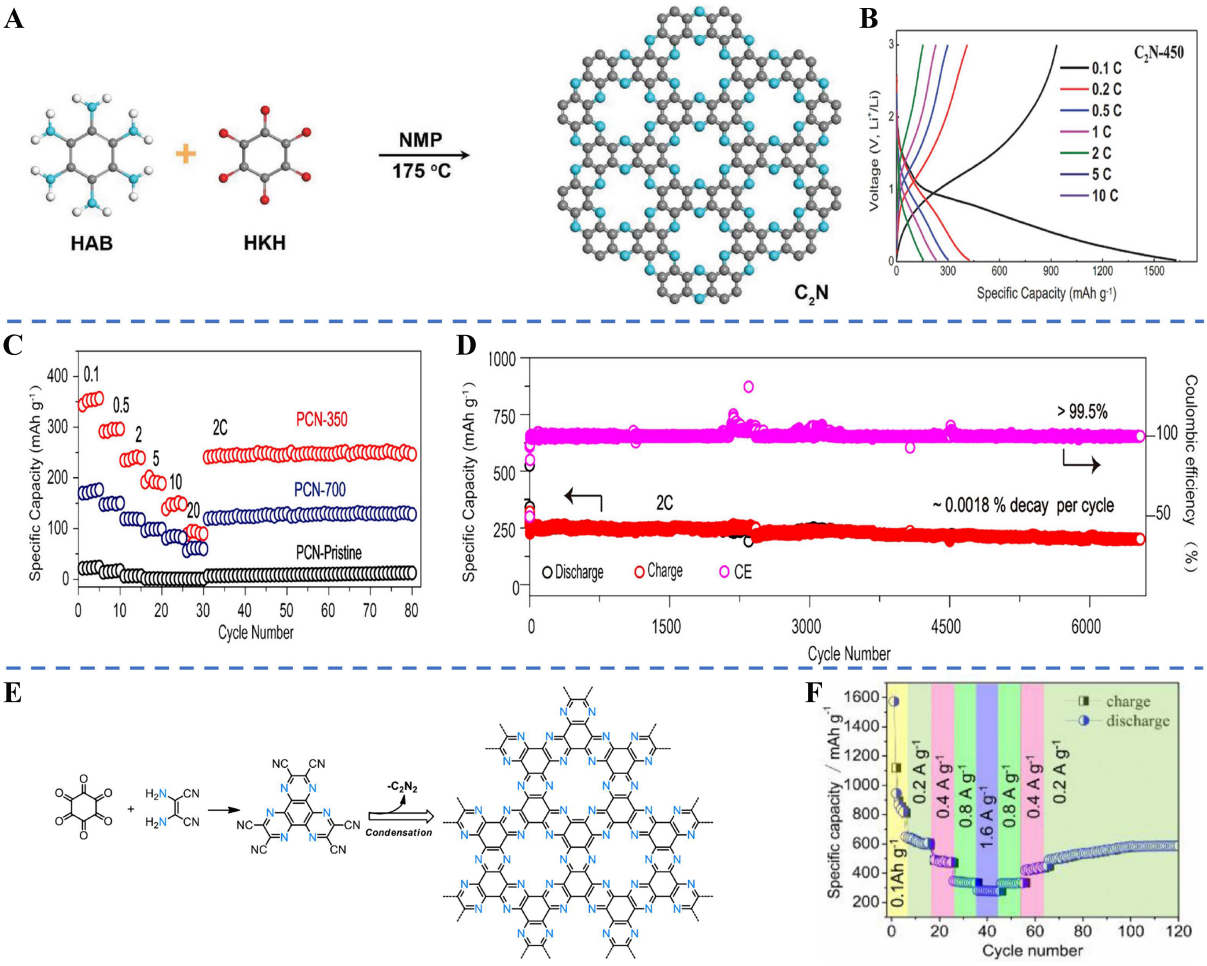

Figure 6. (A) Synthesis of C_2N via wet-chemistry process[54]; (B) Charge and discharge curves of C_2N-450 at various C-rates (1C = 372 mA·g^{-1})[54]; (C) Rate capability test for PCN-350 in SIB (1C = 300 mA·g^{-1})[55]; (D) Cycling stability of the PCN-350 anode (at 600 mA·g^{-1})[55]; (E) Synthesis of C_2N from HAT-CN; (F) Rate performance at different current densities from 0.1 to 1.6 A·g^{-1}[56]. Reproduced from: (A and B) Xu *et al.* (2017), Wiley[54]; (C and D) Yan *et al.* (2022), American Chemical Society[55]; (E and F) Xia *et al.* (2022), ScienceDirect[56]. PCN: Polymeric carbon nitride; SIB: sodium-ion battery; HAT-CN: hexaazatriphenylene-hexacarbonitrile.

bonds adjacent to pyrimidine rings to form TQ-6Li [Figure 9A-D][59]. The terminal phenyl rings were also activated and bound three Li^+ ions to form TQ-9Li. TQ as redox-active units was immobilized into conjugated MOF, resulting in excellent lithium storage capacity.

TQ, as a π-conjugated aromatic species containing C=N and C–N groups, exhibits good redox activity and performance, making it an ideal building block for the construction of polymeric organic electrode materials. Therefore, further research on TQ-based organic electrodes for various metal-ion batteries is of immense practical significance.

Phthalocyanine networks

In 2022, Yang *et al.* prepared two ladder-type crystalline phthalocyanine (Pc) networks (a kind of COF): BB-FAC-Pc-COF and QPP-FAC-Pc-COF, via ortho-dinitrile quadruple condensation of benzo[1,2-b:4,5-b']bis[1,4]benzodioxin-2,3,9,10-tetracarbonitrile (BBTC) and quinoxalino[2',3':9,10]phenanthro[4,5-abc]phenazine-6,7,15,16-tetracarbonitrile (QPPTC) [Figure 10A][60]. The density functional theory (DFT) calculation results suggested four kinds of K^+ adsorption sites in QPP-FACPc-COF around the three kinds

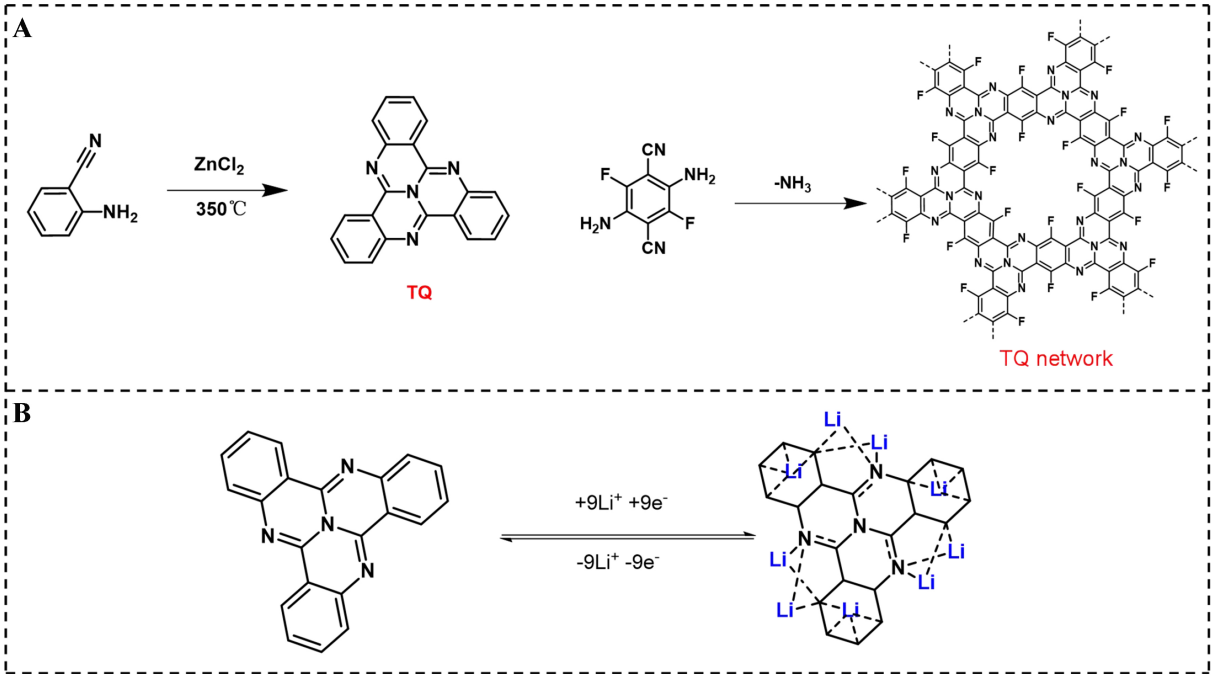

Figure 7. (A) Formation reaction of TQ and TQ networks; (B) Lithium storage mechanism of TQ. TQ: Tricycloquinazoline.

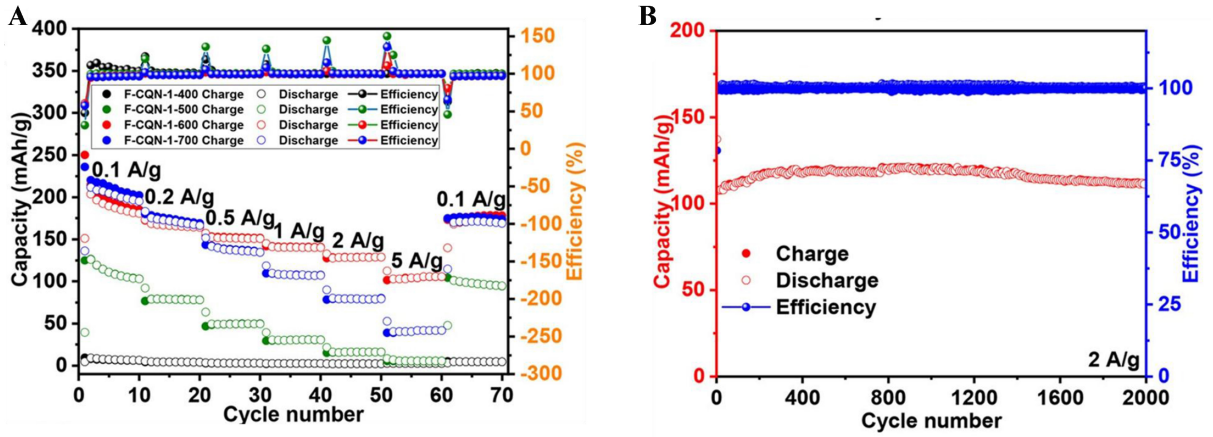

Figure 8. (A) Charge and discharge capacities of F-CQN networks in the LIB half-cells (at 0.1-5.0 A·g^{-1}); (B) Cycling stability of F-CQN-1-600-based LIB half-cell (at 2.0 A·g^{-1})[58]. Reproduced from: Yang *et al.* (2020), American Chemical Society[58]. F-CQN: Fluorinated covalent quinazoline network; LIB: lithium-ion battery.

of N atom and aromatic pyrene moieties [Figure 10B]. Powder X-ray diffraction (PXRD), transmission electron microscopy (TEM), and CO_2 adsorption-desorption isotherm measurements confirmed the presence of tetragonal lattices with a large pore size of 1.6-2.0 nm in these Pc-COFs. The two Pc-COFs showed excellent chemical stability in common solvents and electrolytes. Furthermore, both COFs exhibited high electrical conductivity (0.93-1.94 × 10^{-4} S·cm^{-1}) in the pellet resulting from the full π-conjugation. The use of BB-FAC-Pc-COF and QPP-FAC-Pc-COF as anode materials in PIBs resulted in high reversible capacities of 333 and 424 mAh·g^{-1} at 50 mA·g^{-1} [Figure 10C][60], respectively. Besides, QPP-FAC-Pc-COF showed excellent long-term cycling performance (capacity retention of nearly 100% over 10,000 cycles at 2 A·g^{-1}) [Figure 10D][60]. Owing to their fully conjugated Nitrogen-rich skeleton, porosity, high stability and

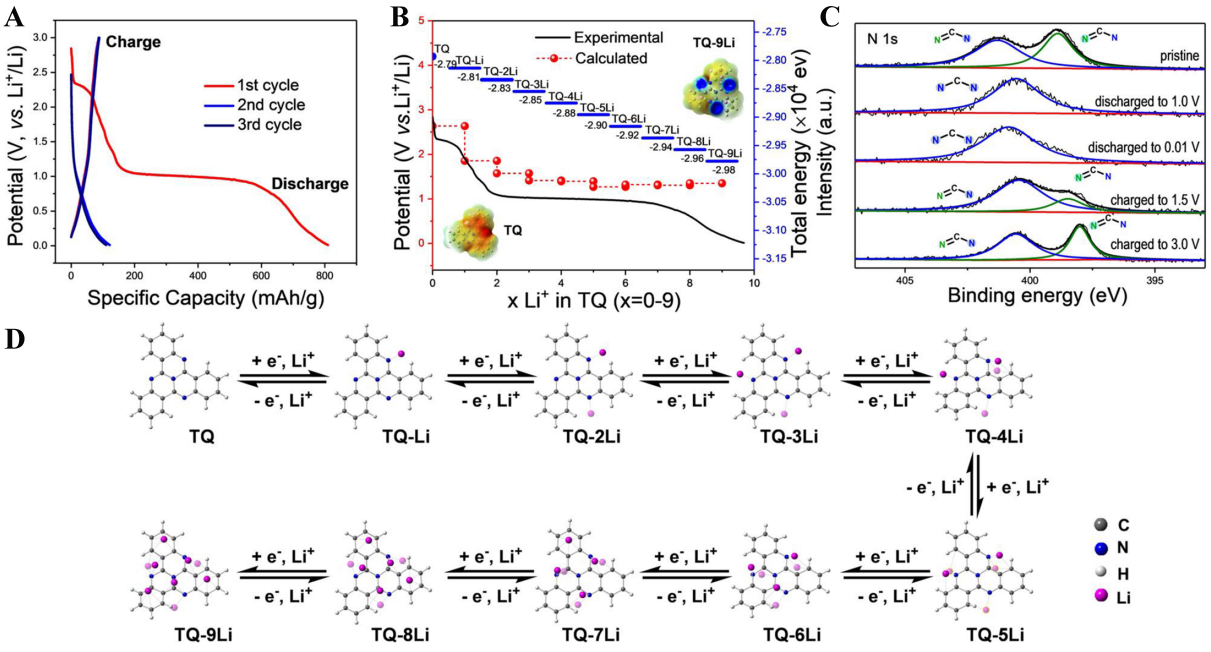

Figure 9. (A) The initial three-cycle charge/discharge profiles of TQ at 30 mA·g^{-1}; (B) The calculated and experimental potential profile of TQ; (C) *Ex situ* XPS spectra of TQ during the charge and discharge state; (D) The calculated lithiation process of TQ in LIBs[59]. Reproduced from: Yan *et al.* (2021), Wiley[59]. TQ: Tricycloquinazoline; XPS: X-ray photoelectron spectroscopy; LIBs: lithium-ion batteries.

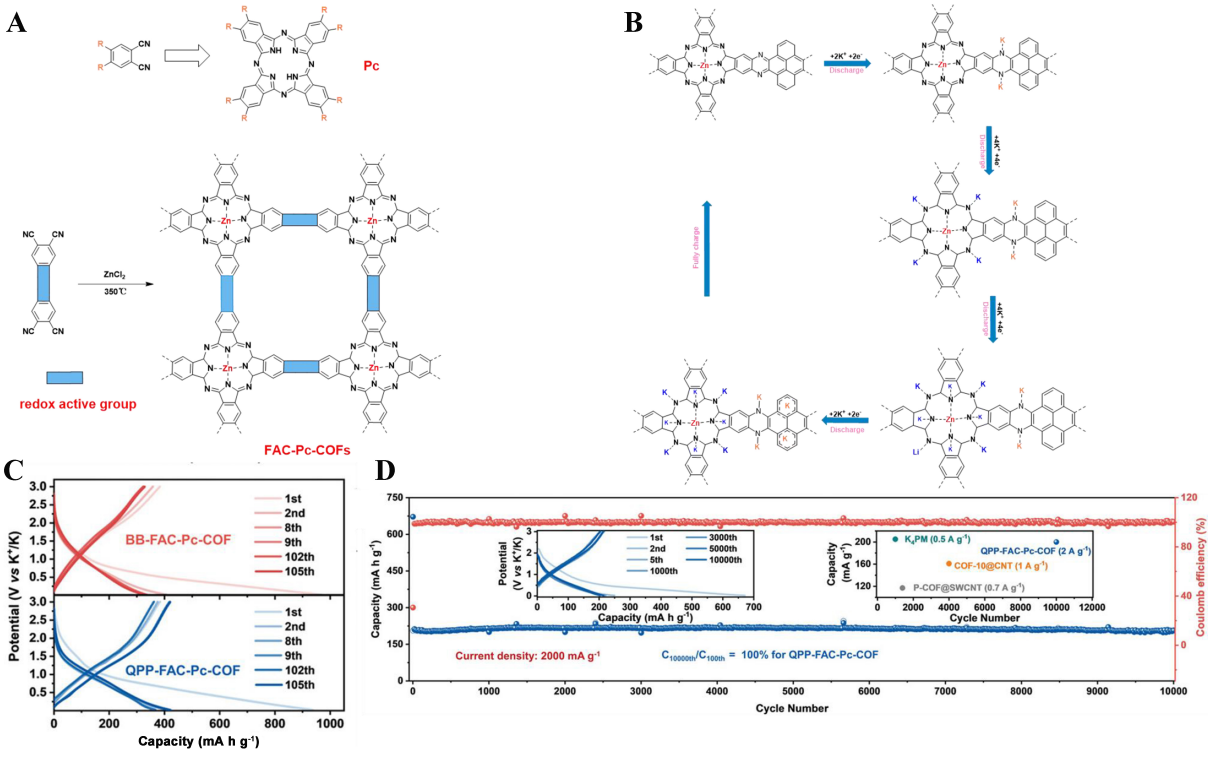

Figure 10. (A) Synthesis of FAC-Pc-COFs; (B) Structural evolution of FAC-Pc-COFs during the potassiation process; (C) Charge and discharge curves of the FAC-Pc-COF for different cycles (at 50 mA·g^{-1})[60]; (D) Long-term cycling stability of the QPP-FAC-Pc-COF (at 2,000 mA·g^{-1})[60]. Reproduced from: Yang *et al.* (2022), Wiley[60]. COFs: Covalent organic framework; QPP: quinoxalino[2′,3′:9,10]phenanthro[4,5-abc]phenazine.

abundant redox-active sites, the Pc-COF anodes displayed high K^+ storage performance in PIBs. Meanwhile, the QPP-FAC-Pc-COF electrode exhibited good Li^+ and Na^+ storage properties, revealing the universal potential of QPP-FAC-Pc-COF as anode materials in various rechargeable batteries.

With the regular dispersion of phthalocyanine as redox-active moieties, the ladder-type covalent networks with phthalocyanine linkage are worth further investigation in various metal-ion batteries. According to the molecular design strategy, the ladder-type phthalocyanine networks with diverse structures can be prepared from different bifunctional ortho-dinitrile precursors[61-65]. It is important to note that similar amorphous materials with phthalocyanine linkage have also been synthesized by the cross-coupling reaction of phthalic anhydride functioned precursor and urea[66].

Benzobisimidazobenzophenathrolinedione networks

Benzobisimidazobenzophenathrolinedione (BBL) and benzobisimidazopyrroloisoindoledione (BPL), obtained from the reaction between 1,8-naphthalic anhydride (phthalic dianhydride) and 1,2-diaminobenzene, are common linkages in linear ladder-type conjugated polymers (LCPs). With high-density C=O, C=N, and C=C groups, BBL and BPL linkages exhibit redox activity, and the corresponding LCPs have gradually emerged as promising and efficient electrode materials for rechargeable batteries[67-71]. Recently, Wang *et al.* reported a ladder-type 2D conjugated COF 2DBBL-TP [Figure 11A], which was employed as an electrode material for fast proton storage in aqueous electrolytes containing Zn^{2+} and strong acids, respectively[71]. The BBL unit underwent two-electron related charge transfer process in which the two C=O groups were reduced to $C–O^-$ in the discharged states [Figure 11B]. The discharged $C–O^-$ groups exhibited reduced basicity owing to the extended π-delocalization in BBL, providing 2DBBL-TP a unique affinity of protons with fast kinetics. In aqueous Zn^{2+} electrolyte (aqueous H_2SO_4 electrolyte), the 2DBBL-TP electrode delivered stable capacities of 65 (71) $mAh·g^{-1}$ at 10 $A·g^{-1}$ with voltage range of 0.3-1.0 V (*vs.* Zn^{2+}/Zn) [-0.3 to 0.3 V (*vs.* Ag/AgCl)] and exhibited excellent cycling stability with 97.2% (almost 100%) capacity retention over 2,000 (10,000) charge-discharge cycles at 10 $A·g^{-1}$ [Figure 11C and D][71]. It is important to note that although C=N and C=C groups of the BBL unit were inert, their redox activity could vary with the backbone structures or the counter-cations[69].

Recently, a series of 2D BBL-based ladder PPNs have been obtained via the polycondensation reaction between 1,4,5,8-naphthalenetetracarboxylic dianhydride and multifunctional ortho-diamine precursors, expanding the material family of BBL networks[72,73]. The redox-active organic molecules, such as phthalocyanine, can be immobilized in the BBL network to form multi-redox active materials, facilitating high-performance electrochemical energy storage[72]. A 2D BPL-based COF structure was synthesized through a process similar to BBL formation, with phthalic acid-functionalized phthalocyanine iron replacing a phthalic dianhydride precursor for condensation polymerization with a 1,2,4,5-tetraaminobenzene derivative[74].

Triphenylene networks

Diels-alder (DA) cycloaddition reaction has been employed for the construction of ladder PPNs benefiting from the simple and catalyst-free aromatic ring formation procedure. Ouyang *et al.* reported the one-pot synthesis of a quinone-enriched ladder PPNs BQ*b*TPL through a modified DA reaction between p-BQ and Hexakis(bromomethyl)benzene (HBB) to form BQ bridged TP linkage [Figure 12A][75]. The unsaturated olefin bonds of BQ and the two adjacent bromomethyl groups underwent [4 + 2] cycloaddition to produce a new benzene ring as ladder-type linkage. Owing to the ladder-type conjugated structure, BQ*b*TPL showed an optical band gap of 1.43 eV and exceptional thermal stability up to 470 °C. The abundant quinone groups serving as redox-active sites [Figure 12B], fully conjugated skeleton, and porous structure make BQ*b*TPL a promising electrode material for LIBs. However, as a large amount of TP worked as linkage but was

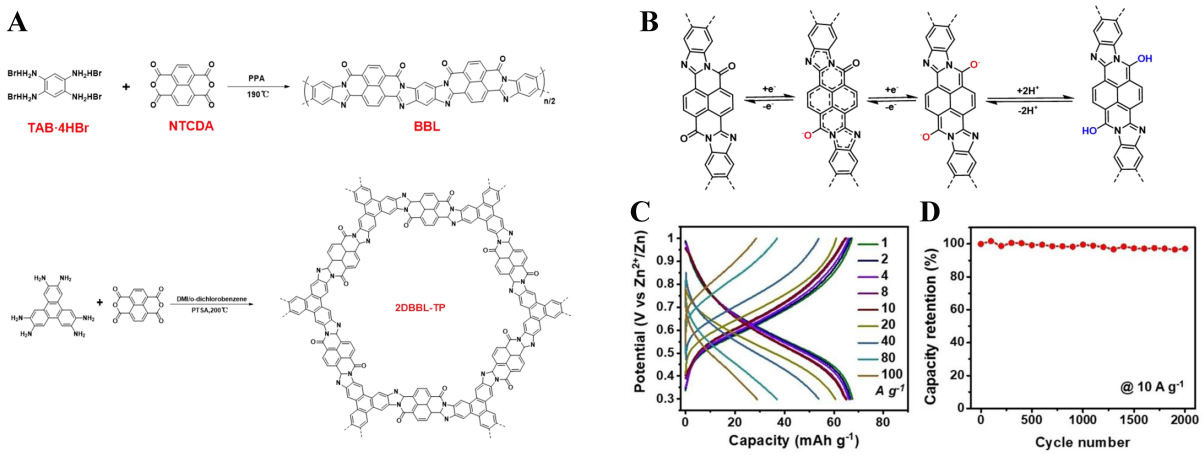

Figure 11. (A) Synthesis and structure of BBL network 2DBBL-TP; (B) Proposed electron-transfer processes for BBL linkage; (C) Rate performance of 2DBBL-TP/CNTs in aqueous $ZnCl_2$ electrolyte at different current densities[71]; (D) Long-term cycling stability of 2DBBL-TP/CNTs[71]. Reproduced from: (C and D) Wang *et al.* (2023), Wiley[71]. BBL: Benzobisimidazobenzophenathrolinedione; TP: triphenylene; CNTs: carbon nanotubes.

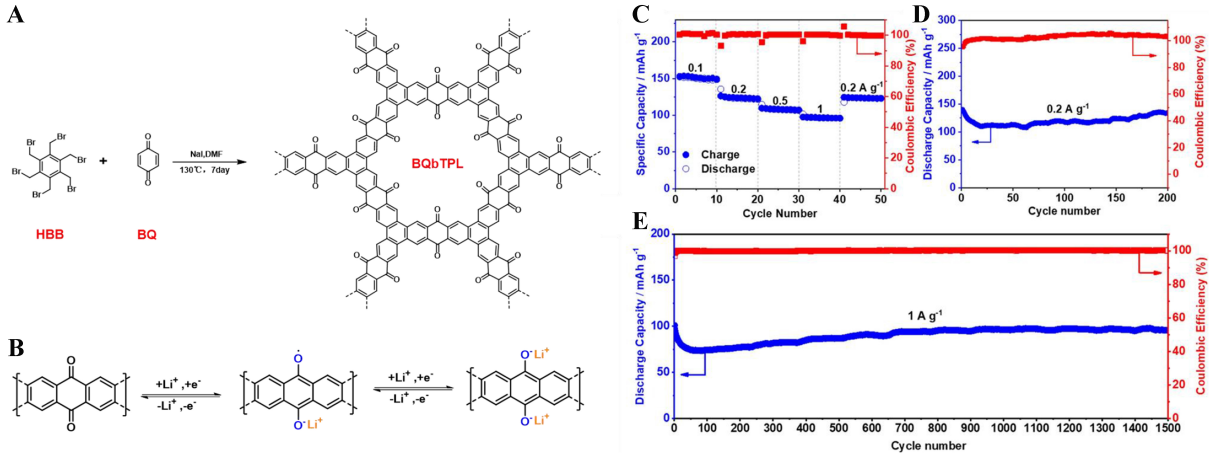

Figure 12. (A) Synthesis and structure of TP network BQ*b*TPL; (B) Lithium storage mechanism of BQ*b*TPL; (C) Rate ability of BQ*b*TPL at various current densities[75]; (D) Cycle performance of BQ*b*TPL at 0.2 A·g^{-1}[75]; (E) Cycling stability of BQ*b*TPL at 1.0 A·g^{-1}[75]. Reproduced from: (C-E) Ouyang *et al.* (2021), American Chemical Society[75]. TP: Triphenylene.

electrochemically inactive, the theoretical capacity of BQ*b*TPL was relatively low (262.7 mAh·g^{-1}). Further, the bandgap of BQ*b*TPL was not narrow enough to ensure high conductivity. A large fraction (40 wt.%) of a conductive carbon additive [multiwalled CNTs (MWCNTs)] was required to prepare the cathode. As a cathode material for LIBs, BQ*b*TPL provided specific capacity of 152.9 mAh·g^{-1} at 0.1 A·g^{-1} (voltage range of 1-3 V *vs.* Li$^+$/Li) [Figure 12C-E][75]. Overall, this DA reaction-based organic approach can be effectively used to construct ladder PPNs materials with redox-active moieties. However, the chemical structures should be designed to increase the electrochemically active parts or activate the TP linkage to ensure high theoretical capacity.

Other polymer networks with potential redox activity

Truxenone is constituted by three fused indanone groups to form a carbonyl-containing aromatic discotic system with electron acceptor character[76]. Due to the redox active C=O groups and activated terminal benzene rings, the truxenone molecule exhibits multi-electron redox reaction activity[77]. Truxenone can

serve as the building block of a COF for the cathode in a solid-state LIB. The truxenone moiety undergoes six-electron transfer during the lithiation/delithiation process [Figure 13A]. After lithiation, six Li^+ ions are loaded around the oxygen atom and the terminal benzene rings are on the truxenone moiety. According to the DFT calculation results, truxenone moiety can host six Li^+ ions within a narrow voltage range during the lithiation process.

Truxenone core is usually synthesized via Aldol triple condensation of 1,3-indanedione derivatives [Figure 13B]. Three aldol reactions occur between the -$COCH_2CO$- groups to form the fused benzene ring in the center. In 2011, Sprick *et al.* synthesized a rigid, microporous, truxenone-cored LCP network through a Lewis acid-assisted cyclotrimerization of bifunctional diketo-s-indacene-type monomers [Figure 13B][78]. The truxenone-cored network was amorphous and displayed a high surface area of 1,650 $m^2 \cdot g^{-1}$. Due to the multifunctional 1,3-indanedione precursor design, Aldol triple condensation is a scalable and facile strategy for the preparation of carbonyl group-rich ladder PPNs.

Tetraoxa[8]circulenes (TOCs) are fused planar aromatic rings, and the cyclooctatetraene core contains three fused benzofuran moieties and can be synthesized by the cyclization of 1,4-naphthoquinone[79]. In 2022, Fritz *et al.* first synthesized a conjugated TOC network [polymeric TOC (pTOC)] via ionothermal approach in eutectic $AlCl_3$/NaCl mixture under a temperature range from 250 to 350 °C [Figure 14][80]. The idealized structure of pTOC showed square 2D lattices with a calculated pore size of ~0.5 nm. The experiential result revealed non-uniform pore size distributions of 0.53, 0.97 nm, and larger pore size ranging from 1.3 to 4 nm in pTOC. The larger micropores and mesopores originated from the overall amorphous structure. The pTOC exhibited an impressive porosity with a high surface area of up to 1,656 $m^2 \cdot g^{-1}$, intrinsic electrical conductivity of 10^{-6}-10^{-5} $S \cdot cm^{-1}$, and excellent thermal stability up to 450 °C, which could facilitate rapid ion and electron transfer kinetics in batteries. The antiaromatic 8 cyclooctatetraene and oxygen-activated phenylene rings were potential redox-active groups, providing high capacity for ions[81-83].

CONCLUSION AND OUTLOOK

Over recent years, the application of organic electrode materials in rechargeable batteries has received considerable research interest, and several organic and polymeric materials have been prepared as high-efficiency electrodes for batteries. In particular, the ladder PPNs materials with inherent electrical conductivity, porosity, rigid backbones, and adjustable redox activity have emerged as a promising platform for organic batteries. Until now, a variety of redox-active ladder PPNs materials have been synthesized and applied as electrode materials in diverse rechargeable batteries. Owing to their extended π-conjugation, which results in long-range charge delocalization and high electrical conductivity, as well as well-defined pore structure that offers efficient ion transport channels, these materials exhibit excellent rate capacities. The rigid backbone with fused rings leads to excellent chemical and thermal stability, which is conducive to long-term cycling stability. The redox-active linkages with numerous redox-active groups ensure high capacity of these materials. Further, the energy storage performance of ladder PPNs can be improved by function-oriented structural design and post-synthetic treatment, such as immobilizing multiple redox-active moieties and annealing procedures. Nevertheless, the wide application of ladder PPNs electrode materials is still hindered by some challenges: (1) The efficient linkage reactions to obtain redox-active ladder PPNs remain limited, and some linkage formation reactions occur at high temperatures, which is not conducive to the low-cost synthesis; (2) The low working potential impedes the construction of high-energy batteries.

For future research, several prospective opportunities may further advance the field of ladder PPNs electrode materials and their applications in organic batteries. For example, new types of ladderization

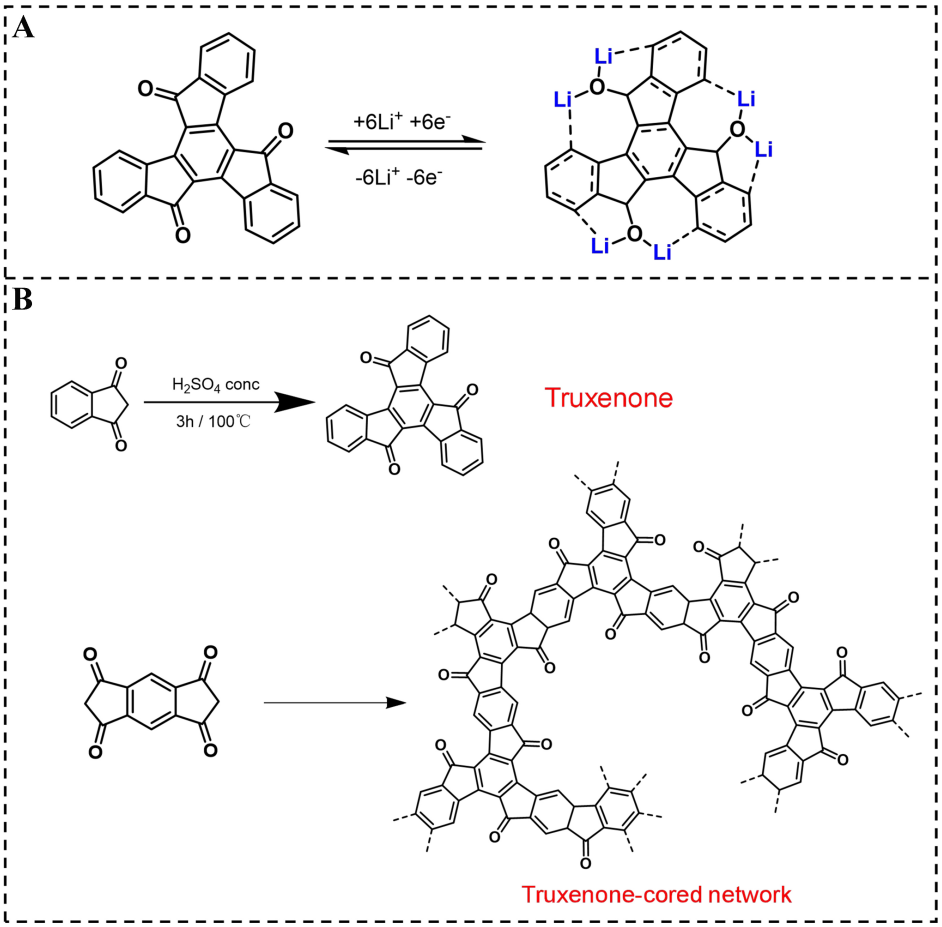

Figure 13. (A) Lithium storage mechanism of truxenone; (B) Synthesis and structure of truxenone-cored network.

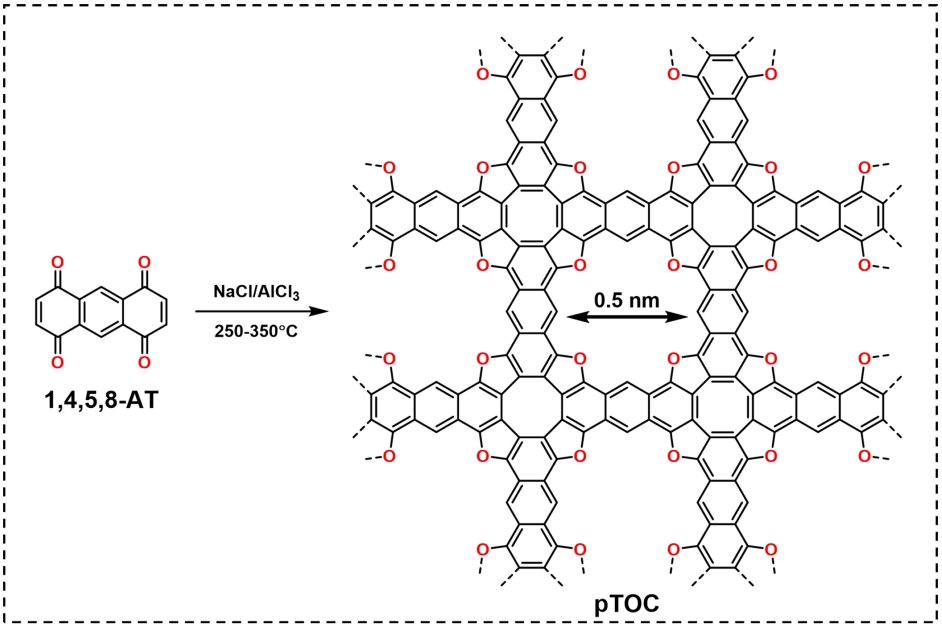

Figure 14. Synthesis and idealized structure of pTOC network. pTOC: Polymeric tetraoxa[8]circulenes.

reactions should be explored to extend the varieties of ladder PPNs. The design and synthesis of novel conjugate monomers with redox activity tailored to specific electrochemical needs may be useful to prepare multifunctional ladder PPNs electrodes for organic batteries. Further research is needed to establish effective structural design strategies for modifying the redox potential and understanding the structure-property relationship. What is more, much easier, more cost-effective and environmentally friendly synthetic routes to monomers, such as synthesis from biomass and avoiding costly precious metal-catalyzed coupling reactions, should be explored to meet the requirement of low-cost practical applications and lessen our carbon footprint. The mild polymeric reaction conditions are also of great importance to large-scale production and application of ladder PPNs. The pore structure of the porous material affects the interactions of the interface between the pore wall and the guest molecules/ions and determines mass transfer efficiency, which is crucial to battery performance. However, the pore engineering of ladder PPNs for high-performance electrode materials has not been well explored. Electrically conductive properties of ladder PPNs are another under-researched area at present. High electrical conductivity facilitates the electron transport to ensure high-rate capability and reduce the amount of conductive additives in batteries. Further study on structural design for conductivity enhancement is required. Overall, the research of ladder PPNs materials is still in its infancy, and further exploration of the structural design and construction, redox activity, and performance improvement is needed to boost their practical applications in rechargeable batteries.

DECLARATIONS

Authors' contributions

Prepared the manuscript: Zhao, C.; Yan, J.
Corrected the manuscript: Ma, Z.; Zhang, Y.
Supervision, funding acquisition, and writing-review: Yan, J.; Hu, T.; Zhang, H.

Availability of data and materials

Not applicable.

Financial support and sponsorship

This work was supported by the National Natural Science Foundation of China (U22A20417, 22393960).

Conflicts of interest

All authors declared that there are no conflicts of interest.

Ethical approval and consent to participate

Not applicable.

Consent for publication

Not applicable.

REFERENCES

1. Kim, J.; Kim, Y.; Yoo, J.; Kwon, G.; Ko, Y.; Kang, K. Organic batteries for a greener rechargeable world. *Nat. Rev. Mater.* **2023**, *8*, 54-70. DOI
2. Xie, J.; Gu, P.; Zhang, Q. Nanostructured conjugated polymers: toward high-performance organic electrodes for rechargeable batteries. *ACS. Energy. Lett.* **2017**, *2*, 1985-96. DOI
3. Lee, S.; Kwon, G.; Ku, K.; et al. Recent progress in organic electrodes for Li and Na rechargeable batteries. *Adv. Mater.* **2018**, *30*,

e1704682. DOI PubMed
4. Lu, Y.; Zhang, Q.; Li, L.; Niu, Z.; Chen, J. Design strategies toward enhancing the performance of organic electrode materials in metal-ion batteries. *Chem* **2018**, *4*, 2786-813. DOI
5. Mauger, A.; Julien, C.; Paolella, A.; Armand, M.; Zaghib, K. Recent progress on organic electrodes materials for rechargeable batteries and supercapacitors. *Materials* **2019**, *12*, 1770. DOI PubMed PMC
6. Xie, J.; Zhang, Q. Recent progress in multivalent metal (Mg, Zn, Ca, and Al) and metal-ion rechargeable batteries with organic materials as promising electrodes. *Small* **2019**, *15*, e1805061. DOI PubMed
7. Chen, Y.; Zhuo, S.; Li, Z.; Wang, C. Redox polymers for rechargeable metal-ion batteries. *EnergyChem* **2020**, *2*, 100030. DOI
8. Poizot, P.; Gaubicher, J.; Renault, S.; Dubois, L.; Liang, Y.; Yao, Y. Opportunities and challenges for organic electrodes in electrochemical energy storage. *Chem. Rev.* **2020**, *120*, 6490-557. DOI PubMed
9. Yin, X.; Sarkar, S.; Shi, S.; et al. Recent progress in advanced organic electrode materials for sodium-ion batteries: synthesis, mechanisms, challenges and perspectives. *Adv. Funct. Mater.* **2020**, *30*, 1908445. DOI
10. Friebe, C.; Schubert, U. S. High-power-density organic radical batteries. *Top. Curr. Chem.* **2017**, *375*, 19. DOI PubMed
11. Wang, D. Y.; Guo, W.; Fu, Y. Organosulfides: an emerging class of cathode materials for rechargeable lithium batteries. *Acc. Chem. Res.* **2019**, *52*, 2290-300. DOI PubMed
12. Häupler, B.; Wild, A.; Schubert, U. S. Carbonyls: powerful organic materials for secondary batteries. *Adv. Energy. Mater.* **2015**, *5*, 1402034. DOI
13. Luo, C.; Borodin, O.; Ji, X.; et al. Azo compounds as a family of organic electrode materials for alkali-ion batteries. *Proc. Natl. Acad. Sci. U. S. A.* **2018**, *115*, 2004-9. DOI PubMed PMC
14. Peng, C.; Ning, G. H.; Su, J.; et al. Reversible multi-electron redox chemistry of π-conjugated N-containing heteroaromatic molecule-based organic cathodes. *Nat. Energy.* **2017**, *2*, 17074. DOI
15. Armand, M.; Grugeon, S.; Vezin, H.; et al. Conjugated dicarboxylate anodes for Li-ion batteries. *Nat. Mater.* **2009**, *8*, 120-5. DOI PubMed
16. Kim, J.; Lee, J.; You, J.; et al. Conductive polymers for next-generation energy storage systems: recent progress and new functions. *Mater. Horiz.* **2016**, *3*, 517-35. DOI
17. Zhang, Z.; Liao, M.; Lou, H.; Hu, Y.; Sun, X.; Peng, H. Conjugated polymers for flexible energy harvesting and storage. *Adv. Mater.* **2018**, *30*, e1704261. DOI PubMed
18. Sun, T.; Xie, J.; Guo, W.; Li, D.; Zhang, Q. Covalent–organic frameworks: advanced organic electrode materials for rechargeable batteries. *Adv. Energy. Mater.* **2020**, *10*, 1904199. DOI
19. Li, J.; Jing, X.; Li, Q.; et al. Bulk COFs and COF nanosheets for electrochemical energy storage and conversion. *Chem. Soc. Rev.* **2020**, *49*, 3565-604. DOI PubMed
20. Sun, H.; Li, J.; Liang, W.; et al. Porous organic polymers as active electrode materials for energy storage applications. *Small. Methods.* **2023**, e2301335. DOI PubMed
21. Luo, D.; Li, M.; Ma, Q.; et al. Porous organic polymers for Li-chemistry-based batteries: functionalities and characterization studies. *Chem. Soc. Rev.* **2022**, *51*, 2917-38. DOI PubMed
22. Lee, J.; Kalin, A. J.; Yuan, T.; Al-Hashimi, M.; Fang, L. Fully conjugated ladder polymers. *Chem. Sci.* **2017**, *8*, 2503-21. DOI PubMed PMC
23. Teo, Y. C.; Lai, H. W. H.; Xia, Y. Synthesis of ladder polymers: developments, challenges, and opportunities. *Chemistry* **2017**, *23*, 14101-12. DOI PubMed
24. Waller, P. J.; Gándara, F.; Yaghi, O. M. Chemistry of covalent organic frameworks. *Acc. Chem. Res.* **2015**, *48*, 3053-63. DOI PubMed
25. Geng, K.; He, T.; Liu, R.; et al. Covalent organic frameworks: design, synthesis, and functions. *Chem. Rev.* **2020**, *120*, 8814-933. DOI PubMed
26. Gui, B.; Ding, H.; Cheng, Y.; Mal, A.; Wang, C. Structural design and determination of 3D covalent organic frameworks. *Trends. Chem.* **2022**, *4*, 437-50. DOI
27. Shi, Y.; Yang, J.; Gao, F.; Zhang, Q. Covalent organic frameworks: recent progress in biomedical applications. *ACS. Nano.* **2023**, *17*, 1879-905. DOI PubMed
28. Wang, C.; Zhang, Z.; Zhu, Y.; Yang, C.; Wu, J.; Hu, W. 2D covalent organic frameworks: from synthetic strategies to advanced optical-electrical-magnetic functionalities. *Adv. Mater.* **2022**, *34*, e2102290. DOI PubMed
29. Zhu, Y.; Xu, P.; Zhang, X.; Wu, D. Emerging porous organic polymers for biomedical applications. *Chem. Soc. Rev.* **2022**, *51*, 1377-414. DOI PubMed
30. Zhang, T.; Xing, G.; Chen, W.; Chen, L. Porous organic polymers: a promising platform for efficient photocatalysis. *Mater. Chem. Front.* **2020**, *4*, 332-53. DOI
31. Yang, D. H.; Tao, Y.; Ding, X.; Han, B. H. Porous organic polymers for electrocatalysis. *Chem. Soc. Rev.* **2022**, *51*, 761-91. DOI PubMed
32. Zhang, Z.; Jia, J.; Zhi, Y.; Ma, S.; Liu, X. Porous organic polymers for light-driven organic transformations. *Chem. Soc. Rev.* **2022**, *51*, 2444-90. DOI PubMed
33. Fajal, S.; Dutta, S.; Ghosh, S. K. Porous organic polymers (POPs) for environmental remediation. *Mater. Horiz.* **2023**, *10*, 4083-138. DOI PubMed

34. Liu, X.; Liu, C. F.; Xu, S.; et al. Porous organic polymers for high-performance supercapacitors. *Chem. Soc. Rev.* **2022**, *51*, 3181-225. DOI PubMed
35. Che, S.; Fang, L. Porous ladder polymer networks. *Chem* **2020**, *6*, 2558-90. DOI
36. Holguin, K.; Mohammadiroudbari, M.; Qin, K.; Luo, C. Organic electrode materials for non-aqueous, aqueous, and all-solid-state Na-ion batteries. *J. Mater. Chem. A.* **2021**, *9*, 19083-115. DOI
37. Yu, Q.; Xue, Z.; Li, M.; et al. Electrochemical activity of nitrogen-containing groups in organic electrode materials and related improvement strategies. *Adv. Energy. Mater.* **2021**, *11*, 2002523. DOI
38. Lu, Y.; Chen, J. Prospects of organic electrode materials for practical lithium batteries. *Nat. Rev. Chem.* **2020**, *4*, 127-42. DOI PubMed
39. Qin, K.; Huang, J.; Holguin, K.; Luo, C. Recent advances in developing organic electrode materials for multivalent rechargeable batteries. *Energy. Environ. Sci.* **2020**, *13*, 3950-92. DOI
40. Zhao, Q.; Zhao, W.; Zhang, C.; et al. Sodium-ion storage mechanism in triquinoxalinylene and a strategy for improving electrode stability. *Energy. Fuels.* **2020**, *34*, 5099-105. DOI
41. Weng, J.; Xi, Q.; Zeng, X.; et al. Recent progress of hexaazatriphenylene-based electrode materials for rechargeable batteries. *Catal. Today.* **2022**, *400-1*, 102-14. DOI
42. Walczak, R.; Kurpil, B.; Savateev, A.; et al. Template- and metal-free synthesis of nitrogen-rich nanoporous "noble" carbon materials by direct pyrolysis of a preorganized hexaazatriphenylene precursor. *Angew. Chem. Int. Ed. Engl.* **2018**, *57*, 10765-70. DOI PubMed
43. Lin, Z.; Xie, J.; Zhang, B.; et al. Solution-processed nitrogen-rich graphene-like holey conjugated polymer for efficient lithium ion storage. *Nano. Energy.* **2017**, *41*, 117-27. DOI
44. Li, X.; Wang, H.; Chen, H.; et al. Dynamic covalent synthesis of crystalline porous graphitic frameworks. *Chem* **2020**, *6*, 933-44. DOI
45. Shehab, M. K.; Weeraratne, K. S.; Huang, T.; Lao, K. U.; El-Kaderi, H. M. Exceptional sodium-ion storage by an aza-covalent organic framework for high energy and power density sodium-ion batteries. *ACS. Appl. Mater. Interfaces.* **2021**, *13*, 15083-91. DOI PubMed
46. Wu, M.; Zhao, Y.; Sun, B.; et al. A 2D covalent organic framework as a high-performance cathode material for lithium-ion batteries. *Nano. Energy.* **2020**, *70*, 104498. DOI
47. Shi, R.; Liu, L.; Lu, Y.; et al. Nitrogen-rich covalent organic frameworks with multiple carbonyls for high-performance sodium batteries. *Nat. Commun.* **2020**, *11*, 178. DOI PubMed PMC
48. Chen, X. L.; Xie, M.; Zheng, Z. L.; et al. Multiple accessible redox-active sites in a robust covalent organic framework for high-performance potassium storage. *J. Am. Chem. Soc.* **2023**, *145*, 5105-13. DOI PubMed
49. Zhang, S.; Zhu, Y. L.; Ren, S.; et al. Covalent organic framework with multiple redox active sites for high-performance aqueous calcium ion batteries. *J. Am. Chem. Soc.* **2023**, *145*, 17309-20. DOI PubMed
50. Wang, J.; En, J. C. Z.; Riduan, S. N.; Zhang, Y. Nitrogen-linked hexaazatrinaphthylene polymer as cathode material in lithium-ion battery. *Chemistry* **2020**, *26*, 2581-5. DOI PubMed
51. Wang, W.; Kale, V. S.; Cao, Z.; et al. Phenanthroline covalent organic framework electrodes for high-performance zinc-ion supercapattery. *ACS. Energy. Lett.* **2020**, *5*, 2256-64. DOI
52. Mahmood, J.; Lee, E. K.; Jung, M.; et al. Nitrogenated holey two-dimensional structures. *Nat. Commun.* **2015**, *6*, 6486. DOI PubMed PMC
53. Meng, L.; Ren, S.; Ma, C.; et al. Synthesis of a 2D nitrogen-rich π-conjugated microporous polymer for high performance lithium-ion batteries. *Chem. Commun.* **2019**, *55*, 9491-4. DOI PubMed
54. Xu, J.; Mahmood, J.; Dou, Y.; et al. 2D frameworks of C_2N and C_3N as new anode materials for lithium-ion batteries. *Adv. Mater.* **2017**, *29*, 1702007. DOI PubMed
55. Yan, J.; Chen, X. L.; Cui, Y.; et al. Engineering microstructure of a robust polymer anode by moderate pyrolysis for high-performance sodium storage. *ACS. Appl. Mater. Interfaces.2022*, 49641-9. DOI PubMed
56. Xia, S.; Cai, Y.; Yao, L.; et al. Nitrogen-rich two-dimensional π-conjugated porous covalent quinazoline polymer for lithium storage. *Energy. Storage. Mater.* **2022**, *50*, 225-33. DOI
57. Buyukcakir, O.; Yuksel, R.; Jiang, Y.; et al. Synthesis of porous covalent quinazoline networks (CQNs) and their gas sorption properties. *Angew. Chem. Int. Ed. Engl.* **2019**, *58*, 872-6. DOI PubMed
58. Yang, Z.; Wang, T.; Chen, H.; et al. Surpassing the organic cathode performance for lithium-ion batteries with robust fluorinated covalent quinazoline networks. *ACS. Energy. Lett.* **2021**, *6*, 41-51. DOI
59. Yan, J.; Cui, Y.; Xie, M.; Yang, G. Z.; Bin, D. S.; Li, D. Immobilizing redox-active tricycloquinazoline into a 2D conductive metal-organic framework for lithium storage. *Angew. Chem. Int. Ed. Engl.* **2021**, *60*, 24467-72. DOI PubMed
60. Yang, X.; Gong, L.; Wang, K.; et al. Ionothermal synthesis of fully conjugated covalent organic frameworks for high-capacity and ultrastable potassium-ion batteries. *Adv. Mater.* **2022**, *34*, e2207245. DOI PubMed
61. Im, Y. K.; Lee, D. G.; Noh, H. J.; et al. Crystalline porphyrazine-linked fused aromatic networks with high proton conductivity. *Angew. Chem. Int. Ed. Engl.* **2022**, *61*, e202203250. DOI PubMed
62. Wei, W. F.; Li, X.; Jiang, K.; Zhang, B.; Zhuang, X.; Cai, T. Exploiting reusable edge-functionalized metal-free polyphthalocyanine networks for efficient polymer synthesis at near infrared wavelengths. *Angew. Chem. Int. Ed. Engl.* **2023**, *62*, e202304608. DOI PubMed
63. Peng, P.; Shi, L.; Huo, F.; et al. In situ charge exfoliated soluble covalent organic framework directly used for Zn-air flow battery. *ACS. Nano.* **2019**, *13*, 878-84. DOI PubMed

64. Zhang, Y.; Zhang, X.; Jiao, L.; Meng, Z.; Jiang, H. L. Conductive covalent organic frameworks of polymetallophthalocyanines as a tunable platform for electrocatalysis. *J. Am. Chem. Soc.* **2023**, *145*, 24230-9. DOI PubMed
65. Wang, Y.; Wang, M.; Chen, T.; et al. Pyrazine-linked iron-coordinated tetrapyrrole conjugated organic polymer catalyst with spatially proximate donor-acceptor pairs for oxygen reduction in fuel cells. *Angew. Chem. Int. Ed. Engl.* **2023**, *62*, e202308070. DOI PubMed
66. Xue, Q.; Xu, Z.; Jia, D.; et al. Solid-phase synthesis porous organic polymer as precursor for Fe/Fe_3C-embedded hollow nanoporous carbon for alkaline oxygen reduction reaction. *ChemElectroChem* **2019**, *6*, 4491-6. DOI
67. Wu, J.; Rui, X.; Wang, C.; et al. Nanostructured conjugated ladder polymers for stable and fast lithium storage anodes with high-capacity. *Adv. Energy. Mater.* **2015**, *5*, 1402189. DOI
68. Fazzi, D.; Negri, F. Addressing the elusive polaronic nature of multiple redox states in a π-conjugated ladder-type polymer. *Adv. Elect. Mater.* **2021**, *7*, 2000786. DOI
69. Yu, J.; Chen, X.; Wang, H.; Gao, B.; Han, D.; Si, Z. Conjugated ladder-type polymers with multielectron reactions as high-capacity organic anode materials for lithium-ion batteries. *Sci. China. Mater.* **2022**, *65*, 2354-62. DOI
70. Ma, T.; Yang, Y.; Johnson, D.; et al. Understanding the mechanism of a conjugated ladder polymer as a stable anode for acidic polymer-air batteries. *Joule* **2023**, *7*, 2261-73. DOI
71. Wang, M.; Wang, G.; Naisa, C.; et al. Poly(benzimidazobenzophenanthroline)-ladder-type two-dimensional conjugated covalent organic framework for fast proton storage. *Angew. Chem. Int. Ed. Engl.* **2023**, *62*, e202310937. DOI PubMed
72. Wang, M.; Fu, S.; Petkov, P.; et al. Exceptionally high charge mobility in phthalocyanine-based poly(benzimidazobenzophenanthroline)-ladder-type two-dimensional conjugated polymers. *Nat. Mater.* **2023**, *22*, 880-7. DOI PubMed PMC
73. Noh, H. J.; Im, Y. K.; Yu, S. Y.; et al. Vertical two-dimensional layered fused aromatic ladder structure. *Nat. Commun.* **2020**, *11*, 2021. DOI PubMed PMC
74. Zhang, Z.; Wang, W.; Wang, X.; Zhang, L.; Cheng, C.; Liu, X. Ladder-type π-conjugated metallophthalocyanine covalent organic frameworks with boosted oxygen reduction reaction activity and durability for zinc-air batteries. *Chem. Eng. J.* **2022**, *435*, 133872. DOI
75. Ouyang, Z.; Tranca, D.; Zhao, Y.; et al. Quinone-enriched conjugated microporous polymer as an organic cathode for Li-ion batteries. *ACS. Appl. Mater. Interfaces.* **2021**, *13*, 9064-73. DOI PubMed
76. Lock, P. E.; Reginato, N.; Bruno-Colmenárez, J.; McGlinchey, M. J. Syntheses, structures and reactivity of metal complexes of trindane, trindene, truxene, decacyclene and related ring systems: manifestations of three-fold symmetry. *Molecules* **2023**, *28*, 7796. DOI PubMed PMC
77. Yang, X.; Hu, Y.; Dunlap, N.; et al. A truxenone-based covalent organic framework as an all-solid-state lithium-ion battery cathode with high capacity. *Angew. Chem. Int. Ed. Engl.* **2020**, *59*, 20385-9. DOI PubMed
78. Sprick, R. S.; Thomas, A.; Scherf, U. Acid catalyzed synthesis of carbonyl-functionalized microporous ladder polymers with high surface area. *Polym. Chem.* **2010**, *1*, 283. DOI
79. Erdtman, H.; Högberg, H. E. Cyclooligomerisation of quinones. *Tetrahedron. Lett.* **1970**, *11*, 3389-92. DOI
80. Fritz, P. W.; Chen, T.; Ashirov, T.; Nguyen, A. D.; Dincă, M.; Coskun, A. Fully conjugated tetraoxa[8]circulene-based porous semiconducting polymers. *Angew. Chem. Int. Ed. Engl.* **2022**, *61*, e202116527. DOI PubMed PMC
81. Chen, F.; Hong, Y. S.; Shimizu, S.; Kim, D.; Tanaka, T.; Osuka, A. Synthesis of a tetrabenzotetraaza[8]circulene by a "fold-in" oxidative fusion reaction. *Angew. Chem. Int. Ed. Engl.* **2015**, *54*, 10639-42. DOI PubMed
82. Kim, J.; Thébault, F.; Heo, M.; et al. 2,3,6,7,10,11-Hexamethoxytriphenylene (HMTP): a new organic cathode material for lithium batteries. *Electrochem. Commun.* **2012**, *21*, 50-3. DOI
83. Chang, Z.; Zhu, M.; Sun, Y.; et al. A conductive 2D conjugated tetrathia[8]circulene-based nickel metal–organic framework for energy storage. *Adv. Funct. Mater.* **2023**, *33*, 2301513. DOI